ORIGINAL ARTICLE

Polymyxin resistance caused by large-scale genomic inversion due to IS26 intramolecular translocation in *Klebsiella pneumoniae*

Haibin Li[a], Lang Sun[a], Han Qiao[a], Zongti Sun[a], Penghe Wang[a], Chunyang Xie[a], Xinxin Hu[a], Tongying Nie[a], Xinyi Yang[a], Guoqing Li[a], Youwen Zhang[a], Xiukun Wang[a], Zhuorong Li[b], Jiandong Jiang[a,c], Congran Li[a,*], Xuefu You[a,*]

[a]*Beijing Key Laboratory of Antimicrobial Agents, Institute of Medicinal Biotechnology, Chinese Academy of Medical Sciences & Peking Union Medical College, Beijing 100050, China*
[b]*Institute of Medicinal Biotechnology, Chinese Academy of Medical Science & Peking Union Medical College, Beijing 100050, China*
[c]*State Key Laboratory of Bioactive Substance and Function of Natural Medicines, Institute of Materia Medica, Chinese Academy of Medical Science & Peking Union Medical College, Beijing 100050, China*

Abstract Polymyxin B and polymyxin E (colistin) are presently considered the last line of defense against human infections caused by multidrug-resistant Gram-negative organisms such as carbapenemase-producer *Enterobacterales*, *Acinetobacter baumannii*, and *Klebsiella pneumoniae*. Yet resistance to this last-line drugs is a major public health threat and is rapidly increasing. Polymyxin S_2 (S_2) is a polymyxin B analogue previously synthesized in our institute with obviously high antibacterial activity and lower toxicity than polymyxin B and colistin. To predict the possible resistant mechanism of S_2 for wide clinical application, we experimentally induced bacterial resistant mutants and studied the preliminary resistance mechanisms. Mut-S, a resistant mutant of *K. pneumoniae* ATCC BAA-2146 (Kpn2146) induced by S_2, was analyzed by whole genome sequencing, transcriptomics, mass spectrometry and complementation experiment. Surprisingly, large-scale genomic inversion (LSGI) of approximately 1.1 Mbp in the chromosome caused by IS26 mediated intramolecular transposition was found in Mut-S, which led to *mgrB* truncation, lipid A modification and hence S_2 resistance. The resistance can be complemented by plasmid carrying intact *mgrB*. The same mechanism was also found in polymyxin B and colistin induced drug-resistant mutants of Kpn2146

*Corresponding authors. Tel.: +86 10 67058991 (Congran Li), +86 10 67061033 (Xuefu You), fax: +86 10 63017302.
E-mail addresses: congranli@imb.pumc.edu.cn (Congran Li), xuefuyou@imb.pumc.edu.cn (Xuefu You).

(Mut-B and Mut-E, respectively). This is the first report of polymyxin resistance caused by IS*26* intramolecular transposition mediated *mgrB* truncation in chromosome in *K. pneumoniae*. The findings broaden our scope of knowledge for polymyxin resistance and enriched our understanding of how bacteria can manage to survive in the presence of antibiotics.

1. Introduction

Polymyxin B and colistin have been used widely for decades to treat serious infections caused by multidrug-resistant Gram-negative organisms. Resistance to polymyxins has been reported in *Klebsiella pneumoniae* by employing several strategies[1]. One common strategy is the modifications of LPS by 4-amino-4-deoxy-L-arabinose (L-Ara4N) and/or phosphoethanolamine (pEtN) to reduce the negative charge. Other mechanisms include the overproduction of surface capsular polysaccharides (CPS)[2] and the released CPS can capture or bind polymyxins, thereby reducing the number of drugs reaching the surface of bacterial cells, resulting in increased polymyxin resistance[3]. LPS modifications involve multiple two-component systems (TCS), including PmrA/PmrB, PhoP/PhoQ and CrrA/CrrB[4]. Meanwhile, PmrA/PmrB controls the *pmrHIJKLM* operon, and PhoP/PhoQ controls the *arnBCADTEF*[5]. The mutations of these TCS and their controlled operons make it easy for bacteria to obtain polymyxin resistance[1,6]. The plasmid-borne MCR-family genes are able to confer colistin resistance by mediating the transfer of pEtN to lipid A[7,8]. MgrB is a small transmembrane protein produced upon activation of the PhoP/PhoQ TCS, and acts as a negative regulator on the system in *K. pneumoniae*[9−11]. A growing number of literatures have reported polymyxin resistance associated with mutations in *mgrB* gene, including insertion of repeat sequences[12], frameshift[13], deletion of the *mgrB* locus[14,15], and premature termination of *mgrB* translation[16]. Particularly, *mgrB* mutation mediated polymyxin resistance related to insertion sequence (IS) is showing an increasing trend in clinical examination[17,18].

The continuous development of genomics has brought great convenience to the study of drug resistance of pathogens[19]. High throughput sequencing technology combined with molecular biology technology has constructed a variety of antibiotic resistance gene databases and analysis tools, which is conducive to us to efficiently find various new drug resistance genes and understand the causes and development process of drug resistance[20]. Besides, transcriptomics and proteomics[21,22] also have potential applications in drug resistance detection, which can correlate genotype data with phenotypic results, especially when genotype and phenotype are inconsistent, or when there is no obvious drug resistance gene but drug resistance has been confirmed[23].

Nephrotoxicity is an important concern with polymyxin use and a common adverse effect clinically[24]. The available polymyxins are complex mixtures, individual constituents may have different pharmacological as well as different toxic effects. Synthesis of individual components and evaluation of their antibacterial activity and renal toxicity are important for new polymyxin development. Previous research in our institute discovered individual component polymyxin S_2, which showed good activity and less toxicity compared with polymyxin B and colistin[25]. High plasma stability *in vitro* and strong efficacy in a mouse systemic infection model (ED_{50} = 0.9 mg/kg) against NDM-1-producing *K. pneumoniae* indicated that polymyxin S2 could be a potential candidate with similar or better antimicrobial potency and lower toxicity than the current clinical polymyxin B and colistin[26]. To predict the possible resistant mechanism of polymyxin S_2 for wide clinical application, we experimentally induced bacterial resistance to polymyxin S_2 and studied the preliminary resistance mechanisms. In this study, we reported the characterization of polymyxin resistant mutants caused by an inversion of approximately 1.1 Mbp in the chromosome by IS*26* mediated intramolecular transposition, which is the first report of polymyxin resistance caused by IS*26* intramolecular transposition mediated *mgrB* truncation in chromosome in *K. pneumoniae*.

2. Materials and methods

2.1. Bacterial strains and growth conditions

Kpn2146 was from the American type culture collection (ATCC); polymyxin S_2-resistant Kpn2146 (Mut-S), polymyxin B-resistant Kpn2146 (Mut-B) and colistin-resistant Kpn2146 (Mut-E) were mutants obtained in our laboratory by polymyxin S_2, polymyxin B and colistin induction respectively. Cation adjusted Muller Hinton II broth (CAMHB) was used for growth of strains in liquid medium, and supplemented with 1.5% agar for growth on solid medium. Unless otherwise indicated, all strains were grown at 37 °C and liquid cultures were additionally shaken at 200 rpm. Growth was monitored by measuring absorbance at 600 nm *via* a spectrophotometer. Bacterial strains were stored in the Collection Center of Pathogen Microorganism of Chinese Academy of Medical Sciences (CAMS-CCPM-A, China). All of the plasmids and strains used in this study are listed in Table 1.

2.2. In vitro induction of polymyxin resistant mutants

Polymyxin S_2 was added to the solid medium with a final concentration of 4 μg/mL. Kpn2146 was then inoculated on the solid media at 2×10^8 CFU/plate. Plates were placed in a constant temperature incubator at 37 °C for about 3 days (up to 7 days) and checked daily to identify spontaneously resistant bacterial subpopulations. The single colonies grew on the plates were isolated, purified on new S_2-containing plates, and preserved. The stability of the drug resistance colonies was detected by passaging on drug-free plate for 3 consecutive days. Mutants (including Mut-S used in the current study) with stable resistance phenotype were stored

Table 1 Plasmids and strains used in this study.

Plasmid or strain	Description	Ref. or source
pCasKP-Apr[a]	Plasmid carrying apramycin resistance gene	27
pTOPO-mgrB (Zeocin)	Plasmid carrying *mgrB* gene and encoding resistance to Zeocin™	This study
pTOPO-mgrB-L (Zeocin)	Plasmid carrying the left half of truncated *mgrB* gene (*mgrB-L*) and encoding resistance to Zeocin™	This study
pTOPO-mdh (Zeocin)	Plasmid carrying *mdh* gene and encoding resistance to Zeocin™	This study
pTOPO-Apr-mgrB	Plasmid carrying *mgrB* gene and encoding resistance to apramycin	This study
pTOPO-Apr-mgrB-L	Plasmids carrying *mgrB-L* and encoding apramycin resistance	This study
pTOPO-Apr-mdh	Plasmid carrying *mdh* gene and encoding resistance to apramycin	This study
pKT25	Plasmid carrying T25 fragment and encoding resistance to kanamycin	Euromedex
pKT25-phoQ	Plasmid carrying *phoQ* gene and encoding resistance to kanamycin	This study
pUT18C	Plasmid carrying T18 fragment and encoding resistance to ampicillin	Euromedex
pUT18C-*mgrB*	Plasmid carrying *mgrB* gene and encoding resistance to ampicillin	This study
pUT18C-*mgrB-L*	Plasmid carrying *mgrB-L* and encoding resistance to ampicillin	This study
pKT25-zip	A derivative of pKT25 in which the leucine zipper of GCN4 is genetically fused in frame to the T25 fragment	Euromedex
pUT18C-zip	A derivative of pUT18C in which the leucine zipper of GCN4 is genetically fused in frame to the T18 fragment	Euromedex
Kpn2146	Wild Type *Klebslela pneumoniae* ATCC BAA2146	ATCC
Mut-S	Kpn2146 mutant obtained by polymyxin S$_2$ induction	This study
Mut-B	Kpn2146 mutant obtained by polymyxin B induction	This study
Mut-E	Kpn2146 mutant obtained by colistin induction	This study
Mut-S (pTOPO-Apr-mgrB)	PMut-S containing pTOPO-Apr-mgrB plasmid	This study
Mut-S (pTOPO-Apr-mgrB-L)	Mut-S containing pTOPO-Apr-mgrB-L plasmid	This study
Mut-S (pTOPO-Apr-mdh)	Mut-S containing pTOPO-Apr-mdh plasmid	This study
Mut-B (pTOPO-Apr-mgrB)	Mut-B containing pTOPO-Apr-mgrB plasmid	This study
Mut-B (pTOPO-Apr-mdh)	Mut-B containing pTOPO-Apr-mdh plasmid	This study
Mut-E (pTOPO-Apr-mgrB)	Mut-E containing pTOPO-Apr-mgrB plasmid	This study
Mut-E (pTOPO-Apr-mdh)	Mut-E containing pTOPO-Apr-mdh plasmid	This study
E. coli BTH101	Reporter strain for BACTH assay	Euromedex
E. coli XL1-Blue	An all-purpose line of competent cells that are ideal for routine cloning needs	Tsingke

[a]Abbreviations: Apr: apramycin resistance.

at $-80\ ^\circ$C for later use. Mut-B and Mut-E were obtained with the same approach.

2.3. Antimicrobial susceptibility assays

Minimum inhibitory concentrations (MICs) were determined using broth microdilution (BMD) method according to EUCAST guidelines[28]. Briefly, fresh bacterial cultures were adjusted to 0.5 McFarland, 1:100 diluted in CAMHB, and inoculated (final inoculate dose of about 5×10^5 CFU/mL) into a 96 well plate containing serial concentrations of polymyxin B, polymyxin S$_2$ or colistin diluted in CAMHB and incubated for 20−24 h at 37 °C. MIC was determined as the lowest concentration that inhibit the growth of the bacteria by naked eyes[29]. *In vitro* polymyxin resistance was defined as an MIC to polymyxin >2 µg/mL according to EUCAST breakpoint[28].

2.4. Detection of mutations in polymyxin resistance related genes

Detection of mutations in polymyxin resistance related genes in Mut-S was performed by PCR in a thermocycler (BioRad, Singapore). Amplicon identity was validated *via* Sanger sequencing. Genomic DNA was extracted with TIANamp Bacteria DNA Kit (Tiangen Biotech, Beijing, China) following the manufacturer's recommendations. The harvested DNA was detected by the agarose gel electrophoresis and quantified by NanoDrop 2000

(Thermo Scientific). All primers were designed using NCBI Primer-BLAST. The PCR reaction volume was 50 µL consisting 25 µL 2 × Phanta® Flash Master Mix (P520, Vazyme Biotech, Nanjing, China), 2 µL each of forward and reverse primers, 19 µL sterile distilled water and 2 µL template DNA. Kpn2146 reference strain was used as a positive control for the investigated genes. Supporting Information Table S1 summarizes sequences of the primers used in this study.

2.5. Isolation and structure characterization of lipid A

Lipid A extraction was performed as described before with some modifications[21,30]. Cell pellets were suspended in PBS, chloroform and methanol were then added to the tube for a single-phase Bligh-Dyer mixture (chloroform:methanol:water, 1:2:0.8, *v/v/v*). After incubating at room temperature for 20 min, pellets were collected and resuspended in hydrolysis buffer (50 mmol/L sodium acetate, pH 4.5; 1% SDS), assisted by sonication at a constant duty cycle for 5 s at 25% output (5 s/burst, ∼5 s between bursts, 5 min in total), then keep in a water bath at 95 °C for 1 h. The SDS solution was converted into a two-phase Bligh-Dyer mixture by adding chloroform and methanol to form a chloroform:methanol:water (2:2:1.8, *v/v/v*) mixture. The lower phases were collected and washed twice with the upper phase of a pre-equilibrated two-phase Bligh-Dyer mixture (2:2:1.8, *v/v/v*), followed by drying under nitrogen. The dried lipids were re-

dissolved in chloroform/MeOH (1:1, *v/v*) and characterized by Triple TOF 5600 (AB Sciex) in negative ion mode.

2.6. RNA sequencing

Wild type (Wt) and Mut-S strains were collected at OD_{600} of 0.4. RNA was isolated using a Bacteria RNA Extraction Kit (R403, Vazyme Biotech, Nanjing, China) in accordance with the manufacturer's instructions. RNA quality was monitored on 1% agarose gels. RNA integrity was assessed using the RNA Nano 6000 Assay Kit of the Bioanalyzer 2100 system (Agilent Technologies, CA, USA). Total RNA was used as input material for the RNA sample preparations. mRNA was purified from total RNA using probes to remove rRNA. Fragmentation was carried out using divalent cations under elevated temperature in First Strand Synthesis Reaction Buffer. First strand cDNA was synthesized using random hexamer primer and M-MuLV Reverse Transcriptase, then use RNaseH to degrade the RNA. And in the DNA polymerase I system, use dUTP to replace the dNTP of dTTPm as the raw material to synthesize the second strand of cDNA. Remaining overhangs were converted into blunt ends *via* exonuclease/polymerase activities. After adenylation of 3′ ends of DNA fragments, adaptors with hairpin loop structure were ligated to prepare for hybridization. Then USER Enzyme was used to degrade the second strand of cDNA containing U. The library fragments were purified with AMPure XP system (Beckman Coulter, Beverly, USA) to select cDNA fragments of preferentially 370−420 bp in length. Then PCR was performed with Phusion High-Fidelity DNA polymerase, Universal PCR primers and Index (X) Primer. At last, PCR products were purified (AMPure XP system) and library quality was assessed on the Agilent Bioanalyzer 2100 system. The clustering of the index-coded samples was performed on a cBot Cluster Generation System using TruSeq PE Cluster Kit v3-cBot-HS (Illumia) according to the manufacturer's instructions. After cluster generation, the library preparations were sequenced on an Illumina Novaseq platform and 150 bp paired-end reads were generated. RNA sequencing was conducted by Illumina Novaseq platform at the Novogene Co., Ltd. (Beijing, China). Differentially expressed genes with a log2 fold change (logFC) of >0 (upregulated expression) or a logFC <0 (down-regulated expression) and a *Q*-value <0.05 were considered significant for this analysis.

2.7. Quantitative PCR with reverse transcription (RT-qPCR)

The extraction method of total RNA was the same as that of transcriptome sequencing. An aliquot (400 ng) of total RNA from each strain was subjected to cDNA synthesis using FastKing RT (with gDNase) (Tiangen, Beijing, China). The cDNAs of *arnA*, *arnB*, *arnC*, *arnD*, *arnF*, *arnT*, *lpxL*, *lpxO*, *lpxT*, *phoP*, *phoQ*, *mgrB*, *eptA*, and 23SrRNA (used as an internal control) were quantified using SuperReal PreMix Plus (SYBR Green) (Tiangen, Beijing, China) and a qTOWER®[3] Real-Time PCR (qPCR) Systems (Analytik Jena, Shanghai, China) according to the manufacturers' instructions. All specific primers (Table S1) were designed according to the genome of Kpn2146 (NCBI reference sequence: NZ_CP006659.2). The relative RNA expression levels were calculated according to the $2^{-\Delta\Delta Ct}$ method with normalization to the 23S rRNA levels. cDNAs were obtained from three independent extractions of mRNA and each one was amplified by RT-qPCR on three independent occasions.

2.8. Genomic sequencing

Bacteria from a single colony were cultured at 37 °C in CAMHB broth and collected at OD_{600} of 0.4. The cells were collected and genomic DNA was extracted using TIANamp Bacteria DNA Kit. The whole genome of wild type and Mut-S were sequenced respectively using Illumina NovaSeq PE150 and PacBio Sequel platform by Beijing Novogene Bioinformatics Technology Co., Ltd. For Illumina NovaSeq PE150 data, SAMTOOLS software (V0.1.18, http://www.htslib.org/)[31] was used to detect the individual SNPs and insertion and deletion of small fragments (<50 bp), as well as the variation analysis of SNP/InDel in the functional regions of the genome. The variation map of the whole genome was created by Circos (V0.64, http://circos.ca/)[32] to show reads coverage and the distribution of SNP and InDel informations. The insertion (INS), deletion (DEL), inversion (INV), intra-chromosomal translocation (ITX), and inter-chromosomal translocation (CTX) between the mutant and wild type strains were analyzed by BreakDancer software (V1.4.4, http://breakdancer.sourceforge.net/)[33]. For PacBio Sequel data, Genome Assembled with SMRT Link software (V5.0.1, https://www.pacb.com/support/software-downloads/) was used. Genomic alignments were performed using the MUMmer (V3.23)[34] and LASTZtools (V1.03.54)[27,35]. Genomic synteny was analyzed based on the alignment results.

2.9. Complementation assays

To determine whether alteration in *mgrB* gene was mediating polymyxin resistance, complementation assay was performed. The full-length *mgrB* gene from polymyxin-susceptible Kpn2146 isolate was amplified by PCR using 2 × Phanta® Flash Master Mix (P510, Vazyme Biotech, Nanjing, China) and primers *mgrB*-ext-F and *mgrB*-ext-R (Table S1). The left half of truncated *mgrB* gene (*mgrB-L*) from polymyxin S₂-resistant Kpn2146 was amplified using the primer *mgrBL-F* and *mgrBL-R*. For construction of the control plasmid, the partial and therefore noncoding *mdh* sequence (full length *mdh* was supposed to encode a malate dehydrogenase[36]) was PCR amplified with primers *mdh*-ext-F and *mdh*-ext-R (Table S1). The amplified fragments were cloned into plasmid pCR™-Blunt II-TOPO® (Invitrogen, Shanghai, China) and the resulting plasmids pTOPO-mgrB (Zeocin), pTOPO-mgrB-L (Zeocin) and pTOPO-mdh (Zeocin) (encoding resistance to Zeocin™) were introduced respectively into *Escherichia coli* TOP10 competent cells (Tsingke Biotechnology, Beijing, China) by chemical transformation. Because Kpn2146 is a multidrug resistant strain[37], and the Mut-S, Mut-B and Mut-E were also resistant to zeocin and kanamycin, the kanamycin-resistant gene of pTOPO (Zeocin) plasmid was replaced by an apramycin-resistant gene for successful selection of plasmid containing colonies. An apramycin resistance cassette (AprR) was amplified from pCasKP[38] using primers ZZ2-F and ZZ2-R, and was ligated into fragments amplified from pTOPO-mgrB (Zeocin), pTOPO-mgrB-L (Zeocin) or pTOPO-mdh (Zeocin) with deletion of kanamycin-resistant gene by primers pCR2-F and pCR2-R (Table S1). The assembly was conducted using Gibson Assembly® Master Mix (NEB, Gene Company, Beijing, China) according to the manufacturer's instructions, and transformed into electrocompetent *E. coli* top10 strains by electroporation. Transformants were selected by overnight incubation at 37 °C on Mueller−Hinton agar supplemented with apramycin (50 µg/mL, MedChemExpress, Shanghai, China). Plasmids were

isolated using the *EasyPure®* Plasmid MiniPrep Kit (Transgen, Beijing, China), confirmed by sequencing, and the correct pTOPO (Apr) plasmids were then introduced into Mut-S, Mut-B and Mut-E respectively by electroporation. The transformants were selected on plates containing 50 μg/mL apramycin and checked by PCR with primer pair pCR2r-F/pCR2r-R (Table S1). The MICs of the transformants for colistin, polymyxin B and polymyxin S_2 were determined.

2.10. Bacterial two-hybrid assays

The two-hybrid assay was performed as reported before[10] following manufacturer's instructions (Euromedex). The genes encoding the proteins of interest (*phoQ* and *mgrB* or *mgrB-L* amplified by PCR using appropriate primers) are sub-cloned into pKT25 and pUT18C vectors in frame with the T25 and T18 fragment open reading frames by using standard molecular biology techniques[39].

The plasmid pKT25-phoQ was constructed by amplifying *phoQ* from Kpn2146 with primers T25-*phoQ*-F and T25-*phoQ*-R, cutting with XbaI and KpnI and ligating into pKT25 by the enzyme sites introduced (XbaI and KpnI). To construct pUT18C-*mgrB*, *mgrB* was amplified from Kpn2146 with primers T18-*mgrB*-F and T18-*mgrB*-R, cut with XbaI and KpnI and ligated into pUT18C cut by the same enzymes. In the same way, to construct pUT18C-*mgrB*-L, *mgrB-L* was amplified from Mut-S with primers T18-*mgrBL*-F and T18-*mgrBL*-R, cut with XbaI and KpnI and inserted pUT18C. Vectors and recombinant plasmids were commonly propagated at 30 °C in standard XL1-Blue strains (Tsingke Biotechnology Co., Ltd.). The recombinant plasmids encoding the T25-phoQ, T18-mgrB and T18-mgrB-L hybrid proteins were then transformed into cyaA2 strain *E. coli* BTH101 competent cells. As a positive control, competent reporter cells should be co-transformed with the control plasmids pKT25-zip and pUT18C-zip. The bacteria are co-transformed with the two recombinant plasmids and plated on either indicator or selective media to reveal the resulting Cya$^+$ phenotype.

The resulted strains to be assayed for β-galactosidase activity were grown in 3 mL LB broth in the presence of 0.5 mmol/L IPTG and appropriate antibiotics (100 μg/mL ampicillin and 50 μg/mL kanamycin) at 30 °C with vigorous agitation overnight (stationary phase). Other steps strictly follow the instruction provided by the Micro β-galactosidase Assay Kit (Beijing Solarbio Science & Technology Co., Ltd.).

2.11. Virulence of the strains in mouse systemic infection model

CD-1 (ICR) mice (19−21 g, half male, half female) were purchased from Vital River Laboratories (Beijing, China). All animals were housed under controlled humidity (30%−70%), temperature (22 ± 3 °C) and a 12 h light−dark cycle. Animals had free access to food and water during the study. All the animal studies complied with the animal husbandry guidelines, and all animal experiments were performed according to national standards for laboratory animals in China (GB/T 35892-2018), with approval from Laboratory Animal Welfare & Ethics Committee in Institute of Medicinal Biotechnology, Peking Union Medical College. Kpn2146, Mut-S, and Mut-S (pTOPO-Apr-mgrB) were subjected to *in vivo* virulence comparison using murine systemic infection model by intraperitoneally injection in the presence of 5% mucin. Cell pellets from fresh overnight cell cultures were properly diluted in saline, and then further 10-fold diluted in 5%

mucin. Four to five infection doses were used for each strain. 0.5 mL of the bacterial suspensions in 5% mucin were injected intraperitoneally to each mouse randomly allocated to different groups. Animal deaths were recorded for 7 days post infection, and the median lethal doses needed to kill 50% of the mice (LD_{50}) and the 95% confidence intervals (CI) were calculated by the Probit method.

2.12. Study on the universality of IS26 intramolecular translocation mediated large-scale genomic inversion in K. pneumoniae

In order to verify whether the new mechanism of polymyxin resistance we found is accidental, we used Kpn2146 and *K. pneumoniae* ATCC 700603 (Kpn700603) strains as the original strains for induction of drug resistant mutants *in vitro* again with the three polymyxin drugs (polymyxin S2, polymyxin B and colistin), and the experiment was repeated three times. For the induced drug-resistant strains, we used two pairs of primers 2146-R-F1/2146-R-R1 and 2146-R-F2/2146-R-R2 (Table S1) to verify whether genome inversion occurred.

2.13. Statistical analysis

Statistical analysis was performed by SPSSv16.0. *P* values were calculated using one-way ANOVA to compare the differences between each pair of groups. $P < 0.05$ was considered statistically significant.

2.14. Accession number(s)

Sequence data from this study were deposited under BioProjects PRJNA779558 (https://www.ncbi.nlm.nih.gov/bioproject/PRJNA779558/), PRJNA947837 (https://www.ncbi.nlm.nih.gov/bioproject/PRJNA947837/), PRJNA947927 (https://www.ncbi.nlm.nih.gov/bioproject/PRJNA947927/), and PRJNA947477 (https://www.ncbi.nlm.nih.gov/bioproject/PRJNA947477/).

3. Results

3.1. Antibacterial susceptibility of Mut-S

As shown in Table 2, Mut-S demonstrated persistent resistance to polymyxins, including polymyxin S_2, polymyxin B and colistin, with MIC values of 16−32 μg/mL, which was 32−64 times higher than those against the susceptible wild type strain (Kpn2146). Further susceptibility test of Mut-S to fourteen antimicrobial agents of different categories demonstrated that Mut-S had similar susceptibility to other antibiotics as the wild type strain except polymyxins (Table 2).

3.2. PCR amplification of polymyxin resistance related genes and second-generation whole genome sequencing of Mut-S

The Mut-S was tested for the presence of gene mutations responsible for resistance to polymyxins in *K. pneumoniae* by PCR and sequencing, the checked genes included *crrB*, *mgrB*, *pmrA*, *pmrB*, *phoP* and *phoQ*. The results demonstrate no mutations in *crrB*, *pmrA*, *pmrB*, *phoP* and *phoQ* (Fig. 1). However, *mgrB* gene cannot be amplified normally even with different primer pairs (*mgrB*-F1/*mgrB*-R1 or *mgrB*-F2/*mgrB*-R2) (Table S1

Table 2 Antimicrobial susceptibility profile of Mut-S in comparison to wild type strain.

Strain	MICs (μg/mL)[a]														
	MEM	CIP	PXS₂	FEP	CTX	CAZ	TET	AMK	PNC	MH	CST	VAN	GEN	ATM	PXB
WT	128	128	0.125	>256	>256	>256	>256	>256	>256	128	0.25	>256	>256	128	0.25
Mut-S	128	128	32	>256	>256	>256	>256	>256	>256	64	32	>256	>256	128	16

Abbreviations: MEM, meropenem; CIP, ciprofloxacin; PXS₂, polymyxin S₂; FEP, cefotaxime; CTX, ceftazidime; CAZ, ceftazidime; TET, tetracycline; AMK, amikacin; PNC, penicillin; MH, minocycline; CST, colistin; VAN, vancomycin; GEN, gentamicin; ATM, aztreonam. PXB, polymyxin B. WT: Wild Type (Kpn2146); Mut-S: Polymyxin S₂-resistant Kpn2146.

[a]MICs (minimum inhibitory concentrations) were determined by broth microdilution method as recommended by CLSI.

and Fig. 1). Mut-S was then subjected to second-generation whole genome sequencing, mapping reads with the reference sequences of Kpn2146 revealed no mutations in polymyxin resistance related genes including *mgrB* (data not shown).

3.3. LPS modification by addition of 4-amino-4-deoxy-larabinose (L-Ara4N) in Mut-S

To examine if polymyxin resistance was related to LPS modifications, we carried out matrix-assisted laser desorption/ionization time-of-flight mass spectrometry (MALDI-TOF) analysis on lipid

A isolated from Mut-S as well as Kpn2146. In wild type strain, normal unmodified lipid A was seen. In contrast, Mut-S demonstrated evidence of modified lipid A with the addition of 4-amino-4-deoxy-L-arabinose (L-Ara4N). The MALDI-TOF spectra of lipid A isolated from wild type strain (Fig. 2A and C) show a dominant peak from hexa-acylated lipid A (mass/charge ratio [*m/z*] of 1841), while the MALDI-TOF spectra of lipid A isolated from Mut-S strain demonstrated an additional peak with *m/z* of 2103 (Fig. 2B and D), indicating modification of lipid A by addition of 2 molecules of L-Ara4N (*m/z* of 131) to the hexa-acylated lipid A.
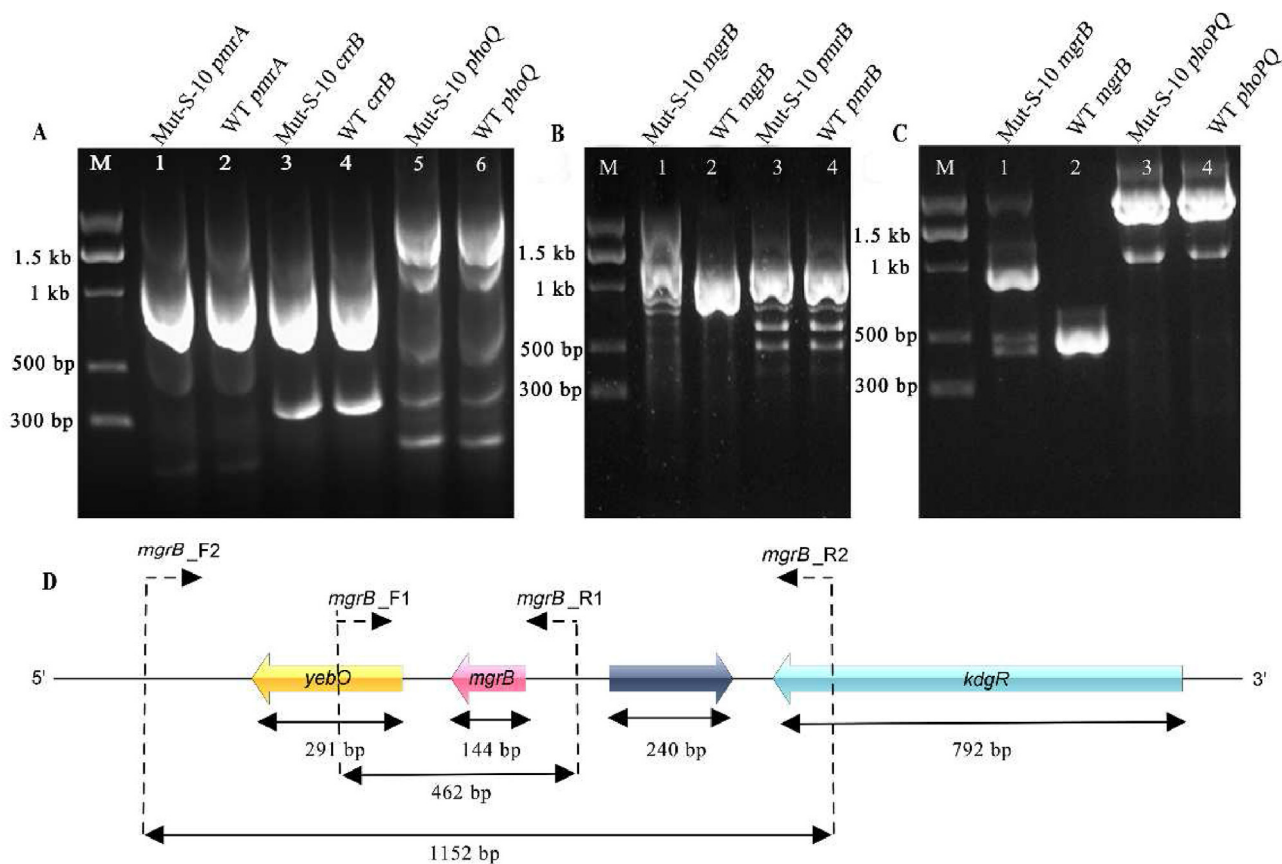
Figure 1 PCR detection of polymyxin resistance-related genes in Mut-S in comparison with Kpn2146. (A) Agarose gel electrophoresis of PCR products of *pmrA*, *crrB*, and *phoQ* genes; (B) Agarose gel electrophoresis of PCR products of *mgrB* gene amplified with primers *mgrB*-F2/*mgrB*-R2 and *pmrB* gene; (C) Agarose gel electrophoresis of PCR products of *mgrB* gene amplified with primers *mgrB*-F1/*mgrB*-R1 and *phoP*, *phoQ* genes. The odd lanes were samples from Mut-S, and the even lanes were samples from wild type strain. (D) The location of primer pairs for amplification of *mgrB* gene on the chromosome.
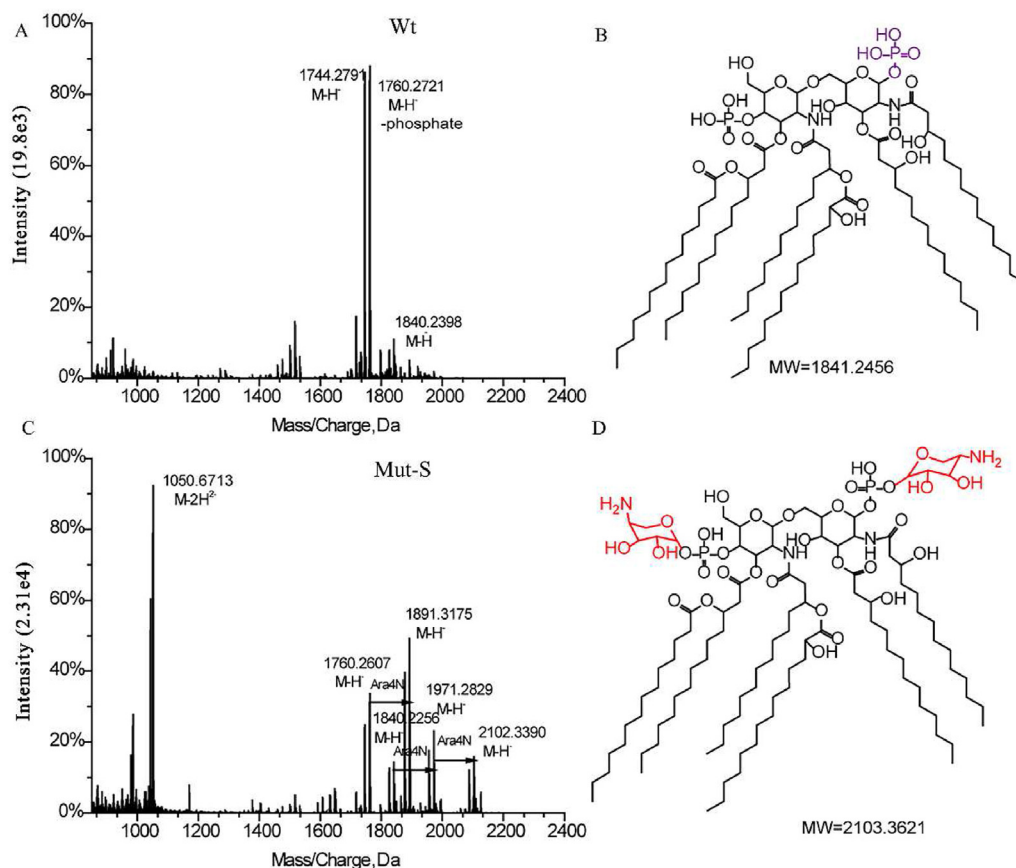
Figure 2 Lipid A modifications in Mut-S in comparison to Kpn2146. MALDI-TOF spectra showing the mass/charge (*m/z*) ratio values of the isolated lipid A. (A) Mass spectroscopy analysis of lipid A from the wild-type strain. (B) Mass spectroscopy analysis of lipid A from Mut-S. Proposed chemical structures of wild type lipid A from Kpn2146 with *m/z* value of 1841 (C) and 4-amino-4-deoxy-L-arabinose modified lipid A from Mut-S with *m/z* value of 2103 (D).

3.4. RNA-Seq of Mut-S and RT-qPCR validation

As LPS modifications were detected, while no gene mutations were found, we went on to check the expression of LPS modification related genes. In RNA-Seq of Mut-S in comparison to wild type strain, a total of 338 differentially expressed genes were detected, including 214 upregulated genes and 124 downregulated genes (Fig. 3). Analysis of genes upregulated in Mut-S showed a significant increase in the expression of the PhoP/PhoQ TCS (2.03-fold for *phoP*, 2.40-fold for *phoQ*, respectively) in comparison to Kpn2146. The gene products of the *arnBCADTEF* operon (also called *pmrHFIJKLM* operon), which is under the positive control of PhoP, demonstrated different degrees of upregulation (2.70−7.52-fold) in Mut-S in comparison to the control. On the contrary, the expression of *mgrB*, a negative regulatory gene of TCS system, which in turn is positively regulated by PhoP/PhoQ, was 0.32-fold downregulated. The expression of the two genes *eptA* and *eptB* responsible for transfer of pEtN to Lipid A was downregulated 0.20- and 0.52-fold, respectively. Other genes upregulated in expression included lipopolysaccharide biosynthesis related gens (*lpxT*, *lpxO*, *lpxL*) and magnesium transporter genes (*mgtC*, *mgtA*) (Supporting Information Table S2). Thirteen genes with significantly altered expression in RNA-seq were selected for further RT-qPCR validation, including upregulated genes (*phoP*, *phoQ*, *arnA*, *arnB*, *arnC*, *arnD*, *arnT*,

arnF, *lpxO*, *lpxL* and *lpxT*) and downregulated genes (*mgrB* and *eptA*). The RT-qPCR values echoed the RNA-seq results (Fig. 4A and B), the expression of *phoP*, *phoQ*, *arnA*, *arnB*, *arnC*, *arnD*, *arnT*, *arnF*, *lpxO*, *lpxL* and *lpxT* were upregulated, while the expression of *mgrB* and *eptA* were downregulated. KEGG is a database resource for understanding high-level functions and utilities of the biological system. We used KOBAS software to test the statistical enrichment of differential expression genes in KEGG pathways. From the results, we concluded that the upregulated genes were mainly enriched in two-component system (kpn02020) and cationic antimicrobial peptide (cAMP) resistance (kpn01503) pathway and the down-regulated genes were also mainly enriched in two-component system (kpn02020). Both KEGG signaling pathways enriched in up-regulated genes contained *phoQ* and *phoP* genes. Hence, our results also suggested that the PhoQ/PhoP signaling system responds to the presence of certain cationic antimicrobial peptides[37]. The PhoQ/PhoP signaling system regulates genes important for growth under these conditions, as well as additional genes important for virulence in many Gram-negative pathogens[10,40,41]. The results also shed light on our subsequent efforts to unravel the mysteries of polymyxin resistance. The differentially expression of genes catalyzing the transfer of L-Ara4N and pEtN to lipid A on lipopolysaccharide surface and mediating polymyxin resistance are summarized in Fig. 4C.
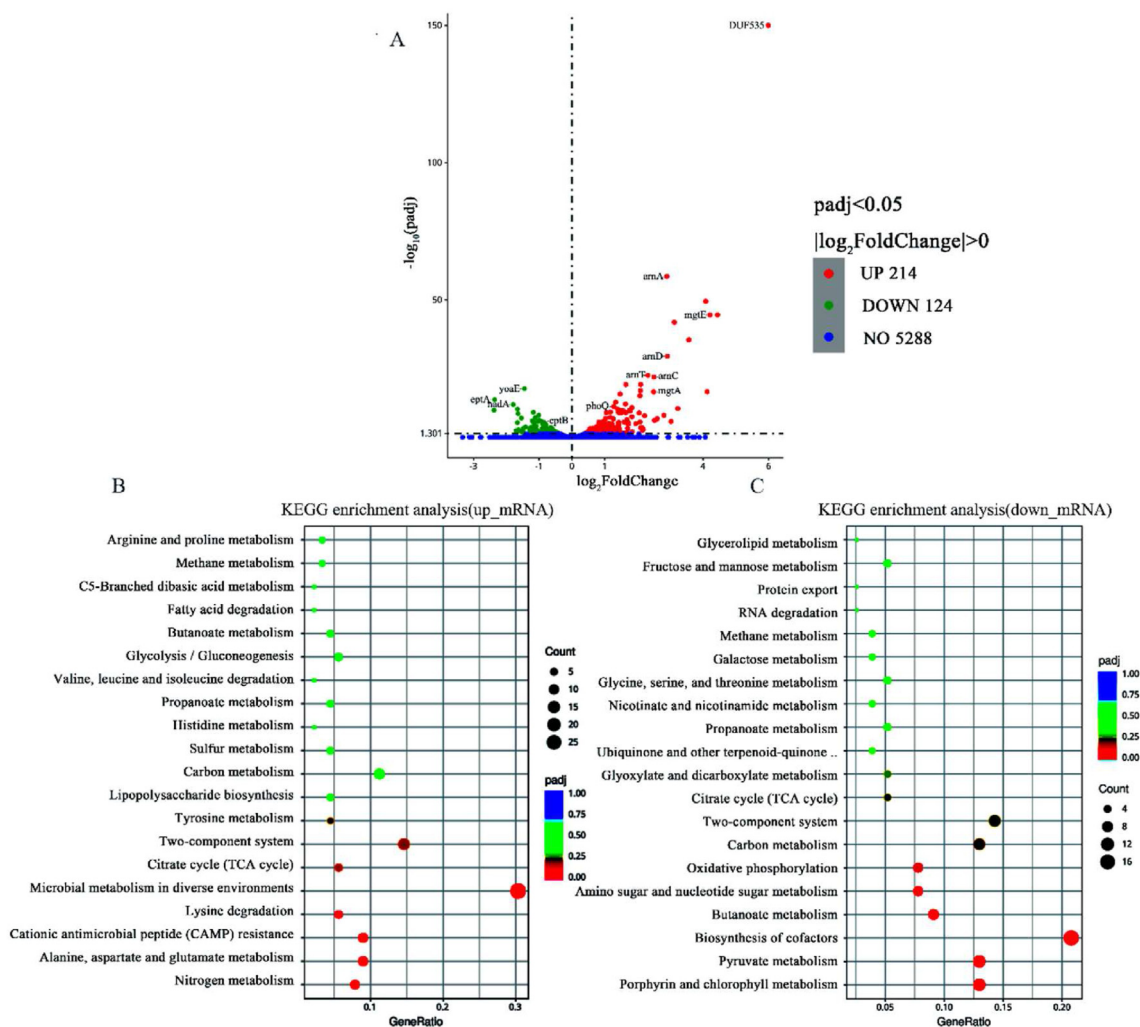
Figure 3 Transcriptome analysis of Mut-S in comparison to Kpn2146. (A) Volcano map displaying the number of upregulated and downregulated genes between Mut-S and the control group. (B) KEGG enrichment analysis of upregulation genes. (C) KEGG enrichment analysis of downregulated genes; the color of the dot represents the size of the P adjust value and the size of the dot represents the number of differential genes.

3.5. Truncation of *mgrB* gene by IS26 mediated intramolecular transposition in Mut-S

The expression changes of LPS modification related genes in Mut-S and no confirmed mutations in the corresponding genes motivated us to try other means. Considering the shortcomings of the second-generation whole genome sequencing, we went with the newer third generation whole genome sequencing (long-read sequencing). Reads were mapped against the reference genome of Kpn2146 (NCBI Reference Sequence: GCA_000364385.3). Surprisingly, comparison of the genomic structure of Mut-S from long-read sequencing with that of the wild type strain revealed an inversion of approximately 1.1 Mbp (Fig. 5). Detailed analysis of the inverted region in Mut-S revealed an IS26 of 820 bp belonging to the IS6 family inside the coding region of *mgrB* gene at nucleotide position 26 (Fig. 6A), which resulted with the disruption of *mgrB* expression. Further examination found the presence of another IS26 downstream of *mgrB* in reverse orientation as the IS26 inside the *mgrB* gene in Mut-S. Besides, in Mut-S, 8 bp

target site duplications (TSD) with reverse orientation were found on both sides of the inverted region, and the 8 bp TSD is right before IS26 on the left side, and right after IS26 on the right side. The arrangement of the sequences suggested the occurrence of intramolecular transposition in the chromosome of Mut-S (Fig. 6B). To confirm the inversion, primers for amplifications of the regions containing the two inversion sites were designed (Table S1) and the amplified PCR products were subjected to Sanger sequencing. The results were consistent with what was found in third generation whole genome sequencing (Fig. 5).

3.6. Susceptibility to polymyxins and confirmation of intramolecular transposition in Mut-B and Mut-S

As shown in Table 3, similar to Mut-S, mutants Mut-B and Mut-E showed consistent resistance to polymyxin S2, polymyxin B and colistin. PCR amplifications of the regions containing the purposed inversion sites also confirmed the inversion of the approximately 1.1 Mbp in Mut-B and Mut-E genome.
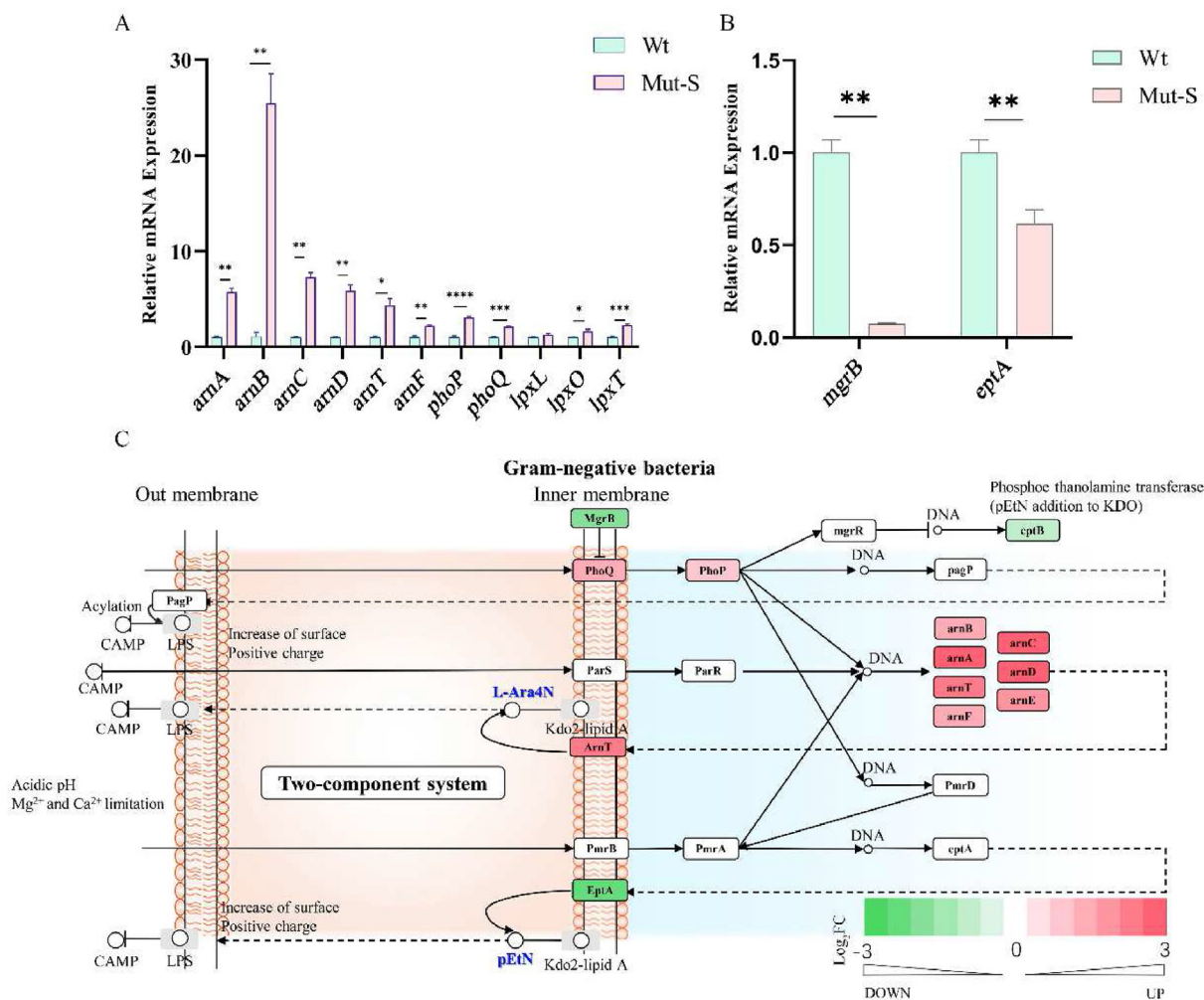
Figure 4 Expression of polymyxin resistance related genes. (A, B) RT-qPCR analysis of the polymyxin resistance related genes. Data are presented as mean ± SD of three independent biological replicates. Wt: wild type strain Kpn2146, Mut-S: Mutant obtained from Kpn2146 by polymyxin S$_2$ induction. *$P < 0.05$, **$P < 0.01$, ***$P < 0.001$. (C) Schematic diagram of the differentially up-regulated and down-regulated genes related to lipid A modification. The diagram was drawn with notations shown in KEGG website (https://www.genome.jp/kegg/document/help_pathway.html).

3.7. Complementation of Mut-S, Mut-B and Mut-E with plasmid carrying mgrB

To further confirm *mgrB* mutation resulted from the inversion of the 1.1 Mbp is the reason for polymyxin resistance in the three mutants, we conducted complementation experiment with recombinant plasmids pTOPO-Apr-mgrB carrying wildtype *mgrB*, pTOPO-Apr-mgrB-L carrying truncated *mgrB* and pTOPO-Apr-mdh carrying a noncoding fragment of *mdh* used as negative control. The plasmids were introduced to the strains by electroporation. As shown in Table 3, Mut-S, Mut-B and Mut-E demonstrated elevated MICs in comparison to the wild type strain, the corresponding strains complemented with pTOPO-Apr-mgrB demonstrated recovery of susceptibility to polymyxins with MICs decreased to the wild type levels. In contrast, transformation with pTOPO-Apr-mdh and pTOPO-Apr-mgrB-L did not restore susceptibility of the strains to polymyxins, with MICs of the related strains similar to the original mutants.

3.8. Bacterial adenylate cyclase two-hybrid system

As expected, cyaA2 strain *E. coli* BTH101 which contained plasmids pKT25 and pUT18C expressing subunits alone (T25 and T18) showed colorless spots on LB-X-Gal plates. The cyaA2 strain BTH101 which contained plasmids pKT25-*phoQ* and pUT18C-*mgrB* expressing fusion proteins (T25-*phoQ* and T18-*mgrB*) showed blue spots on LB-X-Gal plates. The cyaA2 strain BTH101 which contained plasmids pKT25-phoQ and pUT18C-*mgrB*-L expressing fusion protein (T25-phoQ and T18-*mgrB*-L) showed colorless spots on LB-X-Gal plates. The results suggest that wild-type MgrB can interact with PhoQ, whereas the truncated MgrB-L can't (Data not shown).

The efficiency of complementation between the two hybrid proteins was further quantified by assaying the *β*-galactosidase enzymatic activities in bacterial extracts, an easy and robust assay that is correlated with cAMP levels produced in the cells, as the expression of *β*-galactosidase is positively regulated by cAMP/
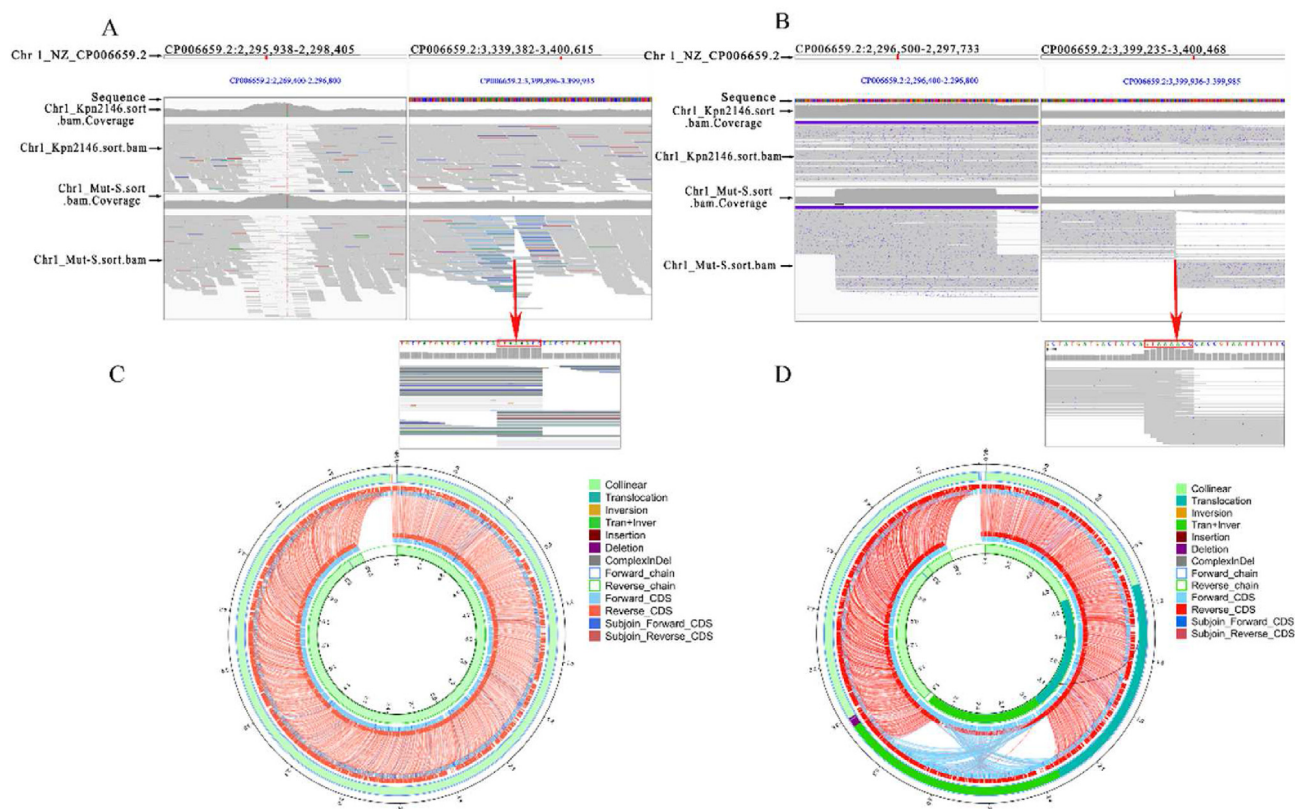
Figure 5 Genomics analysis comparison of Illumina sequencing and long-read sequencing. (A, B) are IGV (v2.11.9) views of part of the Illumina sequencing and long-read sequencing assembly. The red arrow indicates 8 bp direct target site duplication. Each sub-figure represents a region containing inversion sites. Circos plots of the global distribution of genes, SNP variants, and signature are shown in (C) for Illumina sequencing and (D) for long-read sequencing. The inner circle is the sample genome (Mut-S) and the outer circle is the reference genome (Kpn2146).

CAP. The strain expressing T18-MgrB and T25-PhoQ showed a significantly higher level of β-galactosidase activity when compared with strains expressing the T18 and T25 fragments alone or expressing the T18-MgrB-L and T25-PhoQ (Fig. 7), the corresponding β-galactosidase activities were 6329.71 U/mg protein, 792.13 U/mg protein and 733.33 U/mg protein, respectively.

3.9. Polymyxin-resistant mutants (Mut-S) increases virulence

The corresponding LD_{50} values were calculated after mice were sequentially infected with different concentrations of strains [Kpn2146, Mut-S and Mut-S (pTOPO-Apr-mgrB)]. For the WT strain, the LD_{50} value was 4.37×10^5 CFU/mouse, while the LD_{50} value for the Mut-S strain was 2.69×10^5 CFU/mouse. When the Mut-S strain were complemented with the pTOPO-Apr-mgrB plasmid, the LD_{50} value was elevated compared with that before supplementation, being 3.31×10^5 CFU/mouse (Table 4).

3.10. Study on the universality of large-scale genomic inversion

To explore the universality of IS*26* intramolecular translocation mediated large-scale genomic inversion in *K. pneumoniae*, we repeated the *in vitro* resistance induction experiment three more times in the laboratory. Interestingly, we also found different forms of genome segment inversion in polymyxin resistant strains

and the *mgrB* gene was also truncated in different forms compared to WT (Fig. 8A). In the first repeated experiment, we did not find large-scale genomic inversion in the polymyxin S_2 induced drug-resistant strains, but there was large-scale genomic inversion in the polymyxin B and colistin induced drug-resistant strains. The reversed position of its fragment in the polymyxin B induced drug-resistant strains was consistent with the initial findings, and the *mgrB* gene in the colistin induced drug-resistant strains which have large-scale genomic inversion were completely reversed, including 27 bp upstream of the start codon (Fig. 8B); In the second repeated experiment, the strains with large-scale genomic inversion (Mut-S-2, Mut-B-2, Mut-E-2) all had fragment inversion in the same way, *i.e.*, *mgrB-L* included 8 bp upstream of the stop codon of *mgrB* gene (Fig. 8C); In the third repeated experiment, the mutants with fragment inversion occurred in different ways among the resistant strains induced by the three drugs. In the polymyxin S_2 induced resistant strains (Mut-S-3), *mgrB-L* was 57 bp upstream of the stop codon (Fig. 8D). *mgrB-L* differed by 1 bp in polymyxin B induced resistant strains (Mut-B-3) and Colistin induced resistant strains (Mut-E-3), which were 133 and 134 bp upstream of the stop codon, respectively, and the corresponding *mgrB-R* were 11 and 10 bp (Fig. 8E and F). In the three repeated experiments, the three drugs can induce sequence inversions of the same size (such as the results of the second repeated experiment) or different sizes (such as the first and third repeated experiments). The proportion of drug-resistant strains that had large-scale
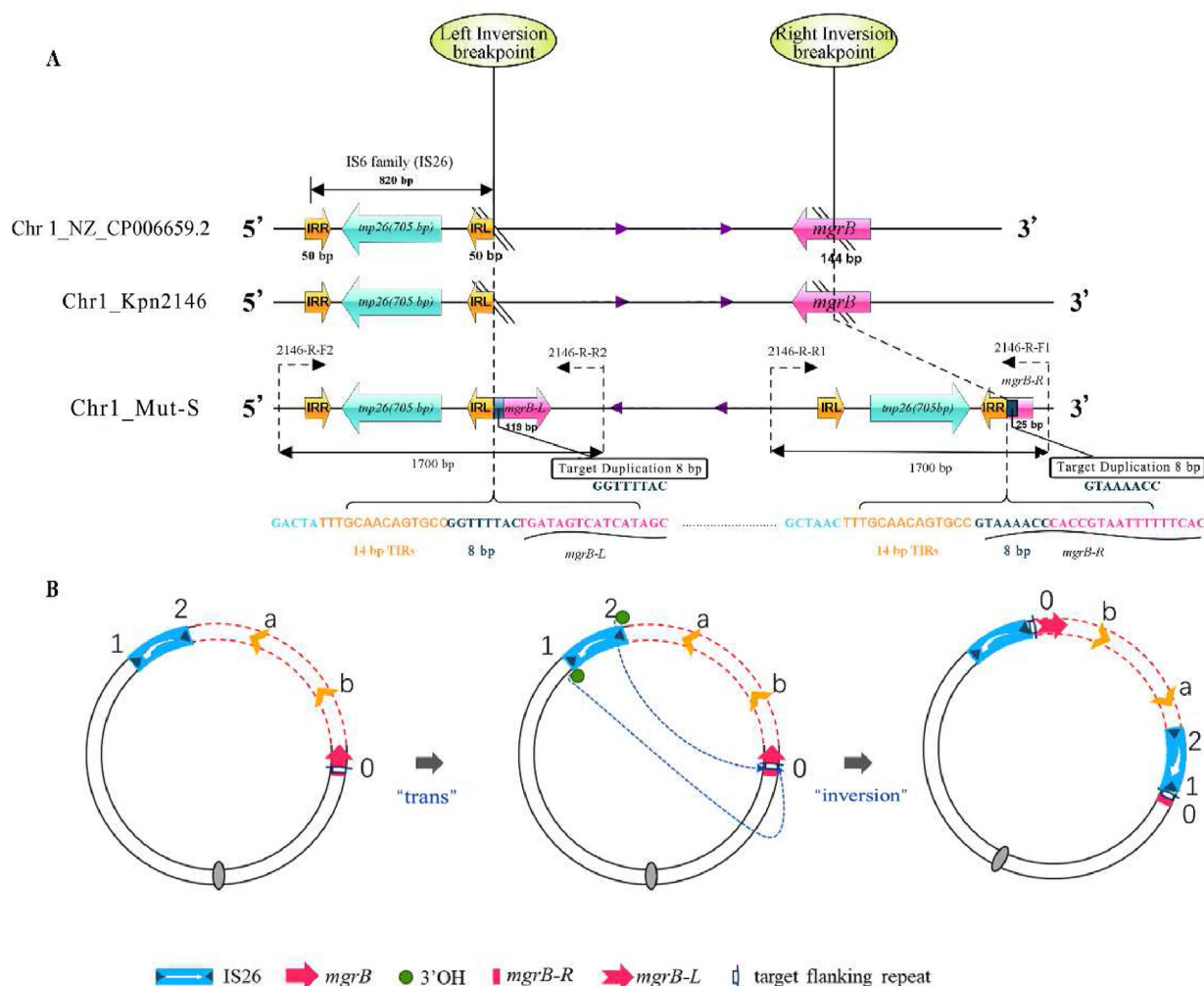
Figure 6 Schematic diagrams of inversion by intramolecular transposition in polymyxin resistant mutants. (A) Genome inversion region in polymyxin resistant strains. Left and right inverted repeats (IRL, IRR) of 14 bp are shown as yellow-filled arrows. The 8 bp direct target site duplications are shown as grey-filled blocks. The transposase open reading frame is shown in blue and its orientation is indicated by the arrowhead. The gene *mgrB* is show in red and its orientation is indicated by the arrowhead. Horizontal lines represent the genome backbone and purple arrow represents the sequence orientation. The positions of primers designed for confirming inversion sites were indicated by dotted lines (2146-R-F1/2146-R-R1 primer pair for one site and 2146-R-F2/2146-R-R2 primer pair for the other site). The schematic diagram was drawn by IBS software (V1.0.3). (B) Schema of intramolecular transposition. The red dotted lines represent the DNA segment between the resident IS and its intramolecular target shown as a while arrow and marked "0". a and b represent two markers on this DNA segment. The 3′-OH groups generated by cleavage at both IS ends can attack the target site on the opposite strand ("trans"). These red arrows represent *mgrB* in different states. The yellow arrow indicates the direction of the genomic DNA sequence. The IS26 is shown as a blue box with the white arrow indicating the direction of expression of the transposase.

genomic inversion in the total acquired drug-resistant strains also varies. In the repeated experiments, mutants with large-scale genomic inversion were all from Kpn2146, while large-scale genomic inversion were not found in Kpn700603 derived mutants of the three experiments.

4. Discussion

In the present study, we demonstrated a novel polymyxin resistance mechanism in *K. pneumoniae* that the inversion of genome sequence mediated by insertion sequence (IS) on bacterial chromosome leads to the truncation of *mgrB* and hence regulation of

antibiotic resistance gene expression, which results with antibiotic resistance. Previous studies suggested that *mgrB* gene is a key target for acquired resistance to colistin in *K. pneumoniae*[42]. Deletion, mutation, and duplication of *mgrB* gene mediate polymyxin resistance. In our study, the *mgrB* gene was divided into two parts by IS26 due to the inversion of genome structure (Fig. 6) and *mgrB* gene expression was downregulated as demonstrated by RNA-Seq and RT-qPCR. Since *mgrB* gene has negative regulation on phoP/phoQ TCS in *K. pneumoniae*[43], *mgrB* down regulation was expected to be associated with overexpression of the phoP/phoQ operon and also of the *arnBCADTEF* operon which is positively regulated by the phoP/phoQ TCS and whose products are eventually responsible for modification of the LPS target.

Table 3 Polymyxin susceptibility of mutants before and after complementation.

| Strain	Chromosomal *mgrB* status	MICs[a] (μg/mL)		
		S₂	PXB	CST
Kpn2146	WT	0.125	0.25	0.25
Mut-S	Interrupted by IS26 element	32	16	32
Mut-S (pTOPO-Apr-mgrB)	Interrupted by IS26 element	0.125	0.25	0.25
Mut-S (pTOPO-Apr-mdh)	Interrupted by IS26 element	32	16	16
Mut-S (pTOPO-Apr-mgrB-L)	Interrupted by IS26 element	32	8	16
Mut-B	Interrupted by IS26 element	32	16	16
Mut-B (pTOPO-Apr-mgrB)	Interrupted by IS26 element	0.125	0.25	0.25
Mut-B (pTOPO-Apr-mdh)	Interrupted by IS26 element	32	8	16
Mut-E	Interrupted by IS26 element	32	16	32
Mut-E (pTOPO-Apr-mgrB)	Interrupted by IS26 element	0.125	0.25	0.25
Mut-E (pTOPO-Apr-mdh)	Interrupted by IS26 element	32	8	32

Abbreviations: S₂, polymyxin S₂; PXB, polymyxin B; CST, colistin; WT, Wild Type strain Kpn2146; Mut-S, Polymyxin S₂-resistant Kpn2146; Mut-B, Polymyxin B-resistant Kpn2146; Mut-E, Colistin-resistant Kpn2146.
[a]MICs (Minimum inhibitory concentrations) were determined by broth microdilution method as recommended by EUCAST.

Indeed, RNA-Seq results and RT-qPCR analysis of the *arnB-CADTEF* operon confirmed the activation of this operon in Mut-S (Fig. 4). The changes of these genes did lead to the modification of lipid A with L-Ara4N moiety of the glycolipid undecaprenyl phosphate-alpha-L-Ara4N as demonstrated by mass detection (Fig. 2). Complementation assays with a plasmid carrying wild type *mgrB* recovered the susceptibility of mutants to polymyxins, while the strains carrying *mgrB-L* did not recovered the susceptibility of mutants to polymyxins. This confirmed the function of

mgrB truncation in mediating polymyxin resistance. However, it is weird that we did not detect the addition of pEtN to lipid A which comprises the second most common alteration underpinning colistin resistance[1], and what's more, the *eptA* gene which is responsible for modification of lipid A by pEtN group, was downregulated. The results may suggest the complexity of regulation of lipid A modification in *K. pneumoniae*, and pEtN modification is less effective than L-Ara4N at increasing the lipid A net charge[44].

The insertion sequence IS26 belonging to the IS6 family, was found in many Gram-negative bacteria as components of both chromosome and plasmids and was known to play a key role in the dissemination of antibiotic-resistance genes[45]. IS26 mediated transfer of resistance genes between plasmids or plasmids and chromosomes has been reported previously[46–48]. IS26 has been shown to form fusions (cointegrates) between two DNA molecules rather than move as a discrete single unit[49]. The IS26 mechanism of movement has long been recognized to be different from the mechanism used by most ISs of different families. IS26 using the replicative mechanism gives rise to deletion or inversion of DNA located between the IS and its target site[50]. In Kpn2146, none of the eleven full copies of IS26, the most frequent IS element in the genome, had the expected 8 bp direct repeat (DR) of the integration target sequence, suggesting that each copy underwent homologous recombination after its last transposition event[37]. Considering the mechanism of IS26 and previous studies[45], we speculate the model of cointegrate formation with duplication of the IS26 and generation of a target duplication in our mutants, *i.e.*, intramolecular transposition. The 3′-OH groups generated by
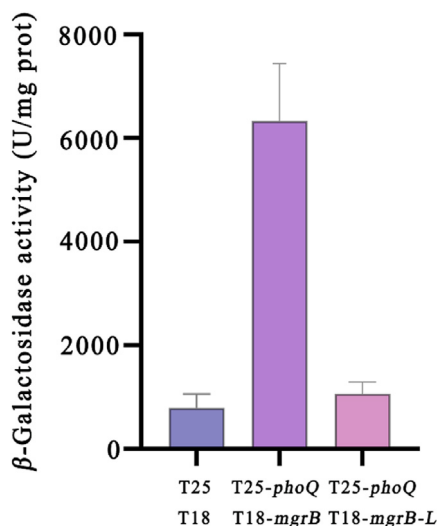
Figure 7 MgrB and MgrB-L interacts with PhoQ. Cells expressed protein fusions to the T18 and T25 subunits of *B. pertussis* adenylyl cyclase. Reconstitution of adenylyl cyclase activity was inferred from beta-galactosidase activity. The control represents cyaA2 strain BTH101 which contained plasmids (pKT25 and pUT18C) expressing subunits alone (T25 and T18). The experimental 1 represents the cyaA2 strain BTH101 which contained plasmids (pKT25-phoQ and pUT18C-*mgrB*) expressing fusion protein (T25-*phoQ* and T18-*mgrB*). The experimental 2 represents the cyaA2 strain BTH101 which contained plasmids (pKT25-*phoQ* and pUT18C-*mgrB*-L) expressing fusion protein (T25-*phoQ* and T18-*mgrB*-L). For each strain, the mean and standard deviation for three independent measurements is shown.

Table 4 Virulence comparison of the strains in mouse systemic infection model.

Strain	LD₅₀ (CFU/ mouse)	95% confidence intervals
Kpn2146	4.37 × 10⁵	2.69 × 10⁵ −7.08 × 10⁵
Mut-S	2.69 × 10⁵	1.12 × 10⁵ −6.76 × 10⁵
Mut-S (pTOPO-Apr-mgrB)	3.31 × 10⁵	1.66 × 10⁵ −6.76 × 10⁵
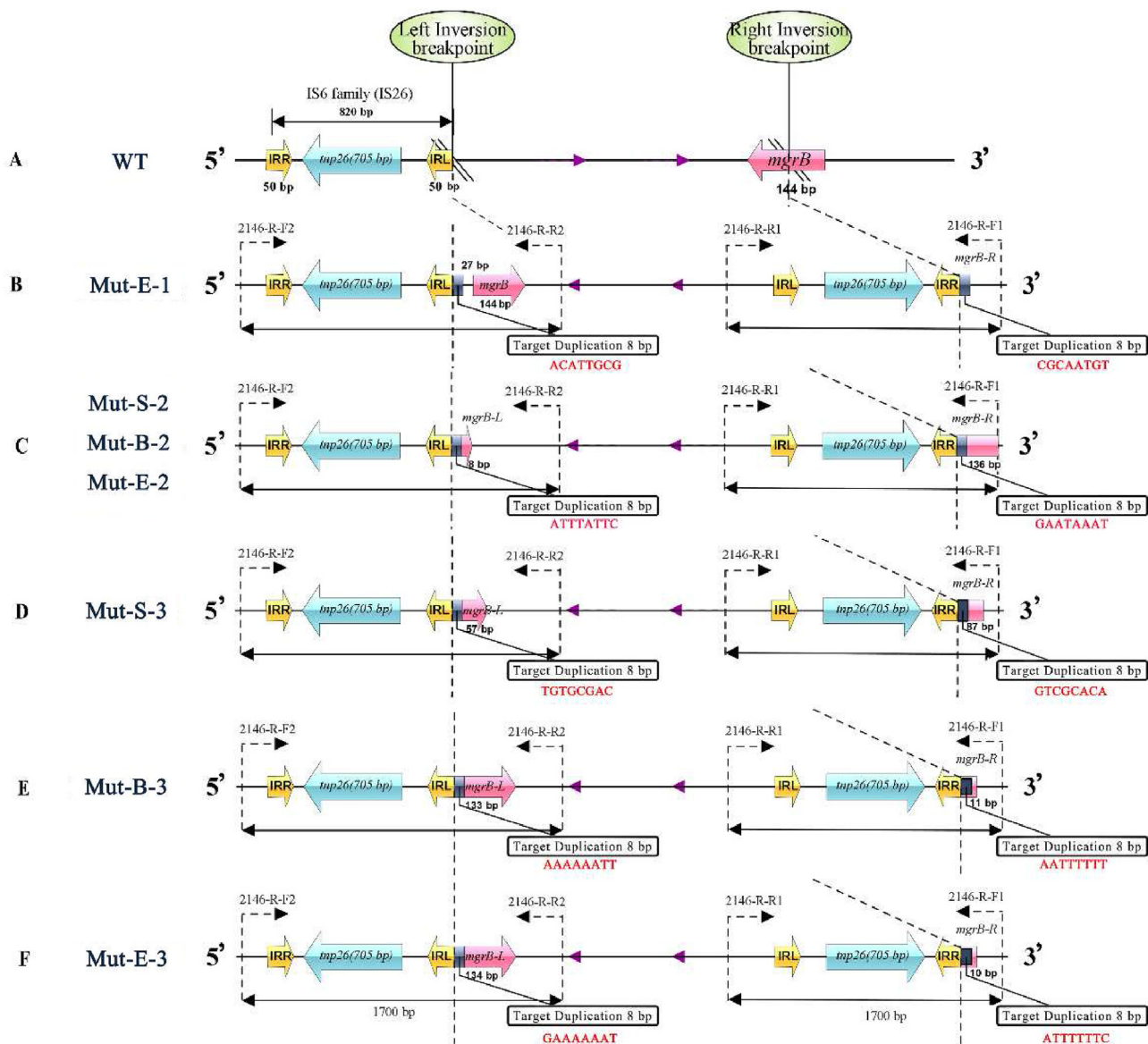
Figure 8 Schematic diagrams of diverse inversion by intramolecular transposition in polymyxin resistant mutants in *Klebsiella pneumoniae*. (A) Partial genome sequence of WT. (B) Schematic diagram of genomic inversion region of colistin induced drug-resistant strains in the first repeated experiment (Mut-E-1). (C) Schematic diagram of genomic inversion region of polymyxins (polymyxin S2, polymyxin B, colistin) induced drug-resistant strains in the second repeated experiment (Mut-S-2, Mut-B-2, Mut-E-2). (D−F) Schematic diagram of genomic inversion region of Polymyxins induced drug-resistant strains in the third repeated experiment (Mut-S-3, Mut-B-3, Mut-E-3).

cleavage at both IS26 ends attack the target site on the opposite strand ("*trans*"). DNA between IS26 and the target site is instead inverted ("*a b*" becomes "*b a*"), bracketed by the original IS and a new copy in an inverted orientation. The target site (an 8 bp region in *mgrB*) is also duplicated but in an inverted orientation, and *mgrB* is truncated into two parts (*mgrB-L* and *mgrB-R*) (Fig. 6). PCR amplification of regions containing the inverted sites in the genomes of Mut-B and Mut-E and verification by sequencing confirmed the same inversion of genome sequence. Further complementation experiment of the three mutants (Mut-S, Mut-B and Mut-E) with a plasmid carrying wildtype *mgrB* confirmed the contribution of *mgrB* truncation (mediated by intramolecular transposition of IS26) to polymyxin resistance. As far as we know, this is the first report that IS26 mediates bacterial resistance to

polymyxin antibiotics through replication and translocation only within the genome of *K. pneumoniae*.

To explore the generality of this polymyxin resistance mechanism in Kpn2146, we reinduced the drug-resistant strains *in vitro* and verified them by PCR amplification. On the basis of the original findings, large-scale genomic inversion at different positions of *mgrB* were detected in polymyxin resistant mutants from Kpn2146 (Supporting Information Table S3). As expected, we did not find large-scale genomic inversion in the Kpn700603 resistant mutants, as its genome does not contain IS26 sequences.

Next-generation sequencing (NGS) was often used to study the mechanism of bacterial drug resistance. Illumina sequencing allows rapid, cheap, and accurate whole genome bacterial analyses, but short reads (<300 base pairs) do not usually enable complete

genome assembly[51]. The *de novo* assembly of short reads results in fragmented assemblies because repetitive sequences in bacterial genomes are invariably longer than the length of a short read and the span of paired-end reads[52]. In the past few years, long-read sequencing technologies have been developed by Pacific Biosciences (PacBio) and Oxford Nanopore Technologies (ONT). Long reads have greater overlap than is provided by short reads, allowing more accurate assemblies, especially in repeat regions. Long-read sequencing offers easier assembly and the ability to span repetitive genomic regions which is the premise of more accurate identification of genomic structural variation[53]. Unfortunately, although these technologies have become available to researchers, it has not been popularized in clinic[54]. In our study, when comparing the Illumina sequencing results with reference gene, the inversion was not found due to the shortcoming of short reads. However, when the long-read sequencing results were compared with the reference gene, the sequence arrangement can be easily elucidated (Fig. 5). Our results strongly demonstrate the advantage of long-read sequencing in detection of bacterial genome structure variation. Therefore, we have reasons to suspect that the clinical isolates that have no confirmed PmrA/B, PhoP/Q or MgrB mutations by Illumina sequencing, but show polymyxin resistance[55−57], may have gene truncation caused by large-scale genomic inversion.

Comparing the Illumina sequencing results with the long-read sequencing results (Fig. 5A and B), a distinctive protrusion of about two-fold higher abundance can be found in the inversion site of *mgrB* in both graphs, indicating the direct target site duplication. This kind of protrusion was hence used for identification of similar inversion in polymyxin resistant *K. pneumoniae*. We first checked whether the genome translocation can happen in other strains using three whole genomes sequenced carbapenem resistant-polymyxin susceptible ATCC strains with annotated IS(s) on the chromosomes [*K. pneumoniae* subsp. pneumoniae ATCC BAA-2470 (Kpn2470), *K. pneumoniae* subsp. pneumoniae ATCC BAA-2472 (Kpn2472) and *K. pneumoniae* ATCC BAA-2473 (Kpn2473)], the three polymyxins (polymyxin S2, polymyxin B and colistin) were again used as the inducer for *in vitro* mutant induction. After several rounds of experiments, 8 mutants from the 3 parental strains were found to have segment inversions manifesting as distinctive protrusions at the supposed target duplication regions, even though the possible relating ISs were different as before (being IS903, ISKpn14, and ISKpn26) (Supporting Information Table S4 and Fig. S1). We further investigated the presence of the mechanism in clinical polymyxin resistant *K. pneumoniae* strains saved in our laboratory. A total of 9 strains demonstrating colistin and polymyxin B resistance were subjected to whole genome sequencing using the PacBio platform and analyzed. However, no segment inversions or even truncations of the *mgrB* gene were found in these clinical isolates (Supporting Information Table S5). We then went on with investigation the presence of the mechanism in clinical polymyxin resistant strains using online database Bacterial and Viral Bioinformatics Resource Center (BV-BRC, Bacterial and Viral Bioinformatics Resource Center)[58], 344 out of 27,134 *K. pneumoniae* isolates were screened out as colistin and/or polymyxin B resistant. Further screening of the 344 isolates with feature: product "mgrB" resulted with 101 strains containing "PhoP/PhoQ regulator MgrB". The gene arrangements of these strains were analyzed, and 18 strains with abnormality in *mgrB* gene assembly and insertion sequence (IS) in the abnormal region were found (Supporting Information Table S6, Fig. S2), which were possible polymyxin

resistant strains caused by IS mediated inversion in *mgrB*. Eight of these strains (*K. pneumoniae* EuSCAPE-TR208, *K. pneumoniae* EuSCAPE_TR232, *K. pneumoniae* Kpngiani7132592, *K. pneumoniae* Kpngiani7132503, *K. pneumoniae* Kpngiani7132624, *K. pneumoniae* Kpngiani7132509, *K. pneumoniae* Kpngiani7132514 and *K. pneumoniae* Kpngiani7132522) with "reads" sequencing data available from SRA (Sequence Read Archive from NCBI, https://www.ncbi.nlm.nih.gov/sra) were subjected to detail analysis by Geneious (version 2023.0), and the distinctive protrusions in *mgrB* coding region were found in all these strains, and the possible related insertion sequences were annotated as IS1 and IS5 (Table S6, Fig. S3). Although more work is required to further characterize these mutants, data presented in this report strongly support the presence of this unique polymyxin resistant mechanism by insertion sequence induced chromosome inversion in *K. pneumonia*e. Whether this mechanism can be applied to other antibiotics and other type of strains remains to be determined.

The bacterial two-hybrid is a rapid genetic approach to detect and characterize interactions between a wide variety of bacterial, eukaryotic, or viral proteins *in vivo*[59]. Euromedex bacterial two-hybrid (BACTH, for "Bacterial Adenylate Cyclase-based Two-Hybrid") system is a simple and fast approach to detect and characterize protein−protein interactions *in vivo*. By bacterial two hybrid system and the subsequent β-galactosidase activity detection experiments, we conclude that the truncated MgrB is unable to exert normal functions. On the other hand, our results also suggested that the N-terminal region of MgrB is a critical part in maintaining its activity, as previously reported that the two N-terminal lysines play an important role in regulating PhoQ activity[60].

Mut-S demonstrated increased virulence in mouse systemic infection model, while complementation of Mut-S with wild type *mgrB* partly lowered the elevated virulence, indicating that *mgrB* mutation participated in mediating the elevated virulence phenotype of Mut-S. It has also been reported that *mgrB* mutation induced PhoPQ-governed lipid A remodeling which confers not only resistance to polymyxins, but also enhances *K. pneumoniae* virulence by decreasing antimicrobial peptide susceptibility and attenuating early host defence response activation[61]. It was then plausible to speculate that the elevated virulence of Mut-S was due to its increased resistance to antimicrobial peptides[61]. This may be a self-protection mechanism that bacteria develop when exposed to antibiotics. Hence, the evidence presented in this work demonstrate that inactivation of *mgrB* not only resulted in polymyxin resistance, but also enhanced *K. pneumoniae* virulence, and highlighted a connection between virulence and antimicrobial resistance.

5. Conclusions

Taken together, we reported the characterization of Kpn2146 polymyxin resistant mutants caused by an inversion of approximately 1.1 Mbp in the chromosome by IS26 mediated intramolecular transposition in *K. pneumoniae* ATCC BAA-2146 in this study. Our results indicate that genome rearrangement due to replicative translocation of IS26 can lead to altered expression of resistance genes, which in turn generates resistance and improves strain virulence. Similar inversions can also be found in clinical polymyxin resistant *K. pneumoniae* and generated by other *K. pneumoniae* strains after induction. A deeper understanding of the resistance of *K. pneumoniae* population to polymyxin antibiotics will be very important for understanding the evolution of polymyxin resistance, for the clinical application of polymyxins and

interpreting public health monitoring data, and for the design and implementation of new control strategies against this important pathogen.

Acknowledgments

Author contributions

Congran Li and Xuefu You initiated and supervised the research. Haibin Li designed and performed the experiments, analyzed the data and wrote the draft manuscript. Han Qiao, and Zongti Sun participated in induction of the drug-resistant mutants. Xiukun Wang, Penghe Wang and Chunyang Xie participated in animal study. Sunlang provided the structure characterization of lipid A. Guoqing Li, Youwen Zhang, Xinxin Hu and Tongying Nie participated in analyzing the data. Congran Li, Xinyi Yang, Xuefu You, Zuorong Li, and Jiandong Jiang revised the manuscript. All authors have read and approved the final version of the manuscript.

Conflicts of interest

The authors declare no conflicts of interest.

Appendix A.   Supporting information

Supporting data to this article can be found online at https://doi.org/10.1016/j.apsb.2023.06.003.

References

1. Olaitan AO, Morand S, Rolain JM. Mechanisms of polymyxin resistance: acquired and intrinsic resistance in bacteria. *Front Microbiol* 2014;**5**:643.
2. Campos MA, Vargas MA, Regueiro V, Llompart CM, Alberti S, Bengoechea JA. Capsule polysaccharide mediates bacterial resistance to antimicrobial peptides. *Infect Immun* 2004;**72**:7107−14.
3. Llobet E, Tomas JM, Bengoechea JA. Capsule polysaccharide is a bacterial decoy for antimicrobial peptides. *Microbiology (Read)* 2008;**154**:3877−86.
4. McConville TH, Annavajhala MK, Giddins MJ, Macesic N, Herrera CM, Rozenberg FD, et al. CrrB positively regulates high-level polymyxin resistance and virulence in Klebsiella pneumoniae. *Cell Rep* 2020;**33**:108313.
5. Mitrophanov AY, Jewett MW, Hadley TJ, Groisman EA. Evolution and dynamics of regulatory architectures controlling polymyxin B resistance in enteric bacteria. *PLoS Genet* 2008;**4**:e1000233.
6. Andrade FF, Silva D, Rodrigues A, Pina-Vaz C. Colistin update on its mechanism of action and resistance, present and future challenges. *Microorganisms* 2020;**8**:176.
7. Liu YY, Wang Y, Walsh TR, Yi LX, Zhang R, Spencer J, et al. Emergence of plasmid-mediated colistin resistance mechanism MCR-1 in animals and human beings in China: a microbiological and molecular biological study. *Lancet Infect Dis* 2016;**16**:161−8.
8. Ling Z, Yin W, Shen Z, Wang Y, Shen J, Walsh TR. Epidemiology of mobile colistin resistance genes *mcr*-1 to *mcr*-9. *J Antimicrob Chemother* 2020;**75**:3087−95.
9. Olaitan AO, Diene SM, Kempf M, Berrazeg M, Bakour S, Gupta SK, et al. Worldwide emergence of colistin resistance in *Klebsiella pneumoniae* from healthy humans and patients in Lao PDR, Thailand, Israel, Nigeria and France owing to inactivation of the PhoP/PhoQ regulator *mgrB*: an epidemiological and molecular study. *Int J Antimicrob Agents* 2014;**44**:500−7.
10. Lippa AM, Goulian M. Feedback inhibition in the PhoQ/PhoP signaling system by a membrane peptide. *PLoS Genet* 2009;**5**:e1000788.
11. Cannatelli A, Giani T, D'Andrea MM, Di Pilato V, Arena F, Conte V, et al. MgrB inactivation is a common mechanism of colistin resistance in KPC-producing *Klebsiella pneumoniae* of clinical origin. *Antimicrob Agents Chemother* 2014;**58**:5696−703.
12. da Silva KE, Thi Nguyen TN, Boinett CJ, Baker S, Simionatto S. Molecular and epidemiological surveillance of polymyxin-resistant *Klebsiella pneumoniae* strains isolated from Brazil with multiple *mgrB* gene mutations. *Int J Med Microbiol* 2020;**310**:151448.
13. Nishida S, Ono Y. Genomic analysis of a pan-resistant *Klebsiella pneumoniae* sequence type 11 identified in Japan in 2016. *Int J Antimicrob Agents* 2020;**55**:105854.
14. Song Y, Yang J, Ju Y, Liu D, Wang Y, Sun X, et al. Genomic insights into a complete deletion of the *mgrB* locus in colistin-resistant *Klebsiella pneumoniae* ST2268 isolated from a human infection. *J Glob Antimicrob Resist* 2021;**27**:75−8.
15. de Araujo Longo LG, Fontana H, Santos de Sousa V, Chilinque Zambao da Silva N, Souto Martins I, Meurer Moreira B. Emergence of *mgrB* locus deletion mediating polymyxin resistance in pandemic KPC-producing *Klebsiella pneumoniae* ST15 lineage. *J Med Microbiol* 2021;**70**:001309.
16. Kong Y, Li C, Chen H, Zheng W, Sun Q, Xie X, et al. *In vivo* emergence of colistin resistance in carbapenem-resistant *Klebsiella pneumoniae* mediated by premature termination of the *mgrB* gene regulator. *Front Microbiol* 2021;**12**:656610.
17. Hamel M, Chatzipanagiotou S, Hadjadj L, Petinaki E, Papagianni S, Charalampaki N, et al. Inactivation of *mgrB* gene regulator and resistance to colistin is becoming endemic in carbapenem-resistant *Klebsiella pneumoniae* in Greece: a nationwide study from 2014 to 2017. *Int J Antimicrob Agents* 2020;**55**:105930.
18. Huang PH, Cheng YH, Chen WY, Juan CH, Chou SH, Wang JT, et al. Risk factors and mechanisms of *in vivo* emergence of colistin resistance in carbapenem-resistant *Klebsiella pneumoniae*. *Int J Antimicrob Agents 2021;57:106342*.
19. Loman NJ, Pallen MJ. Twenty years of bacterial genome sequencing. *Nat Rev Microbiol* 2015;**13**:787−94.
20. Bakour S, Sankar SA, Rathored J, Biagini P, Raoult D, Fournier PE. Identification of virulence factors and antibiotic resistance markers using bacterial genomics. *Future Microbiol* 2016;**11**:455−66.
21. Sun L, Rasmussen PK, Bai Y, Chen X, Cai T, Wang J, et al. Proteomic changes of *Klebsiella pneumoniae* in response to colistin treatment and *crrB* mutation-mediated colistin resistance. *Antimicrob Agents Chemother* 2020;**64**:e02200−19.
22. Jasim R, Baker MA, Zhu Y, Han M, Schneider-Futschik EK, Hussein M, et al. A comparative study of outer membrane proteome between paired colistin-susceptible and extremely colistin-resistant *Klebsiella pneumoniae* strains. *ACS Infect Dis* 2018;**4**:1692−704.
23. Boolchandani M, D'Souza AW, Dantas G. Sequencing-based methods and resources to study antimicrobial resistance. *Nat Rev Genet* 2019;**20**:356−70.
24. Ouderkirk JP, Nord JA, Turett GS, Kislak JW. Polymyxin B nephrotoxicity and efficacy against nosocomial infections caused by multiresistant Gram-negative bacteria. *Antimicrob Agents Chemother* 2003;**47**:2659−62.
25. Cui AL, Hu XX, Gao Y, Jin J, Yi H, Wang XK, et al. Synthesis and bioactivity investigation of the individual components of cyclic lipopeptide antibiotics. *J Med Chem* 2018;**61**:1845−57.
26. Cui AL, Hu XX, Chen Y, Jin J, Yi H, Wang XK, et al. Design, synthesis, and bioactivity of cyclic lipopeptide antibiotics with varied polarity, hydrophobicity, and positive charge distribution. *ACS Infect Dis* 2020;**6**:1796−806.

27. Chiaromonte F, Yap VB, Miller W. Scoring pairwise genomic sequence alignments. *Pac Symp Biocomput* 2002;**7**:115−26.

28. The European Committee on Antimicrobial Susceptibility Testing. Breakpoint tables for interpretation of MICs and zone diameters. Version 12.0. 2022. Available from: http://www.eucast.org.

29. Wang Q, Lv Y, Pang J, Li X, Lu X, Wang X, et al. *In vitro* and *in vivo* activity of D-serine in combination with β-lactam antibiotics against methicillin-resistant *Staphylococcus aureus*. *Acta Pharm Sin B* 2019;**9**:496−504.

30. Henderson JC, O'Brien JP, Brodbelt JS, Trent MS. Isolation and chemical characterization of lipid A from Gram-negative bacteria. *J Vis Exp* 2013;**16**:e50623.

31. Li H, Handsaker B, Wysoker A, Fennell T, Ruan J, Homer N, et al. The sequence alignment/map format and SAMtools. *Bioinformatics* 2009;**25**:2078−9.

32. Krzywinski M, Schein J, Birol I, Connors J, Gascoyne R, Horsman D, et al. Circos: an information aesthetic for comparative genomics. *Genome Res* 2009;**19**:1639−45.

33. Chen K, Wallis JW, McLellan MD, Larson DE, Kalicki JM, Pohl CS, et al. BreakDancer: an algorithm for high-resolution mapping of genomic structural variation. *Nat Methods* 2009;**6**:677−81.

34. Kurtz S, Phillippy A, Delcher AL, Smoot M, Shumway M, Antonescu C, et al. Versatile and open software for comparing large genomes. *Genome Biol* 2004;**5**:R12.

35. Harris RS. *Improved pairwise alignment of genomic DNA*. Ph.D. Thesis. Philadelphia: College of Engineering, Pennsylvania State University; 2007.

36. Diancourt L, Passet V, Verhof J, Grimont PA, Brisse S. Multilocus sequence typing of *Klebsiella pneumoniae* nosocomial isolates. *J Clin Microbiol* 2005;**43**:4178−82.

37. Hudson CM, Bent ZW, Meagher RJ, Williams KP. Resistance determinants and mobile genetic elements of an NDM-1-encoding *Klebsiella pneumoniae* strain. *PLoS One* 2014;**9**:e99209.

38. Wang Y, Wang S, Chen W, Song L, Zhang Y, Shen Z, et al. CRISPR-Cas9 and CRISPR-assisted cytidine deaminase enable precise and efficient genome editing in. *Klebsiella pneumoniae*. *Appl Environ Microbiol* 2018;**84**. 018344-e1918.

39. Green MR, Sambrook J. Molecular Cloning, A Laboratory Manual, 4th ed., Cold Spring Harbor Protocols. Available from: http://molecularcloning.com/index.php.

40. Xu Q, Xu T, Zhuang Y, Liu X, Li Y, Chen Y. *In vivo* development of polymyxin B resistance in *Klebsiella pneumoniae* owing to a 42 bp deletion in the sequence of phoQ. *BioMed Res Int* 2020;**2020**:5868479.

41. Groisman EA. The pleiotropic two-component regulatory system PhoP-PhoQ. *J Bacteriol* 2001;**183**:1835−42.

42. Poirel L, Jayol A, Bontron S, Villegas MV, Ozdamar M, Turkoglu S, et al. The *mgrB* gene as a key target for acquired resistance to colistin in *Klebsiella pneumoniae*. *J Antimicrob Chemother* 2015;**70**:75−80.

43. Cannatelli A, D'Andrea MM, Giani T, Di Pilato V, Arena F, Ambretti S, et al. *In vivo* emergence of colistin resistance in *Klebsiella pneumoniae* producing KPC-type carbapenemases mediated by insertional inactivation of the PhoQ/PhoP *mgrB* regulator. *Antimicrob Agents Chemother* 2013;**57**:5521−6.

44. Elias R, Duarte A, Perdigao J. A molecular perspective on colistin and *Klebsiella pneumoniae*: mode of action, resistance genetics, and phenotypic susceptibility. *Diagnostics* 2021;**11**:1165.

45. Varani A, He S, Siguier P, Ross K, Chandler M. The IS*6* family, a clinically important group of insertion sequences including IS*26*. *Mobile DNA* 2021;**12**:11.

46. Wan M, Gao X, Lv L, Cai Z, Liu JH. IS*26* mediates the acquisition of tigecycline resistance gene cluster *tmexCD1-toprJ1* by IncHI1B-FIB plasmids in *Klebsiella pneumoniae* and *Klebsiella quasipneumoniae* from food market sewage. *Antimicrob Agents Chemother* 2021;**65**. 021788-20.

47. Yang X, Ye L, Li Y, Chan EW, Zhang R, Chen S. Identification of a chromosomal Integrated DNA fragment containing the *rmpA2* and *iucABCDiutA* virulence genes in *Klebsiella pneumoniae*. *mSphere* 2020;**5**:011799-20.

48. Takeuchi D, Akeda Y, Yoshida H, Hagiya H, Yamamoto N, Nishi I, et al. Genomic reorganization by IS*26* in a *bla*NDM-5-bearing FII plasmid of *Klebsiella pneumoniae* isolated from a patient in Japan. *J Med Microbiol* 2018;**67**:1221−4.

49. Harmer CJ, Hall RM. An analysis of the IS*6*/IS*26* family of insertion sequences: is it a single family?. *Microb Genom* 2019;**5**:e000291.

50. Harmer CJ, Moran RA, Hall RM. Movement of IS*26*-associated antibiotic resistance genes occurs *via* a translocatable unit that includes a single IS*26* and preferentially inserts adjacent to another IS26. *mBio* 2014;**5**:e01801−14.

51. De Maio N, Shaw LP, Hubbard A, George S, Sanderson ND, Swann J, et al. Comparison of long-read sequencing technologies in the hybrid assembly of complex bacterial genomes. *Microb Genom* 2019;**5**: e000294.

52. Liao YC, Cheng HW, Wu HC, Kuo SC, Lauderdale TY, Chen FJ. Completing circular bacterial genomes with assembly complexity by using a sampling strategy from a single MinION Run with barcoding. *Front Microbiol* 2019;**10**:2068.

53. Schatz M. *De novo* assembly of complex genomes using single molecule sequencing. Available from: http://schatzlab.cshl.edu/presentations/2014-01-14.PAG.Single%20Molecule%20Assembly.pdf.

54. Ameur A, Kloosterman WP, Hestand MS. Single-Molecule Sequencing: towards clinical applications. *Trends Biotechnol* 2019;**37**: 72−85.

55. Jayol A, Poirel L, Dortet L, Nordmann P. National survey of colistin resistance among carbapenemase-producing *Enterobacteriaceae* and outbreak caused by colistin-resistant OXA-48-producing *Klebsiella pneumoniae*, France, 2014. *Euro Surveill* 2016;**21**:30339.

56. Poirel L, Jayol A, Nordmann P. Polymyxins: antibacterial activity, susceptibility testing, and resistance mechanisms encoded by plasmids or chromosomes. *Clin Microbiol Rev* 2017;**30**:557−96.

57. Luo Q, Yu W, Zhou K, Guo L, Shen P, Lu H, et al. Molecular epidemiology and colistin resistant mechanism of *mcr*-positive and *mcr*-negative clinical isolated. *Escherichia coli*. *Front Microbiol* 2017; **8**:2262.

58. Olson RD, Assaf R, Brettin T, Conrad N, Cucinell C, Davis JJ, et al. Introducing the Bacterial and Viral Bioinformatics Resource Center (BV-BRC): a resource combining PATRIC, IRD and ViPR. *Nucleic Acids Res* 2023;**51**:D678−89.

59. Karimova G, Pidoux J, Ullmann A, Ladant D. A bacterial two-hybrid system based on a reconstituted signal transduction pathway. *Proc Natl Acad Sci U S A* 1998;**95**:5752−6.

60. Yadavalli SS, Goh T, Carey JN, Malengo G, Vellappan S, Nickels BE, et al. Functional determinants of a small protein controlling a broadly conserved bacterial sensor kinase. *J Bacteriol* 2020;**202**:e00305−20.

61. Kidd TJ, Mills G, Sá-Pessoa J, Dumigan A, Frank CG, Insua JL, et al. A *Klebsiella pneumoniae* antibiotic resistance mechanism that subdues host defences and promotes virulence. *EMBO Mol Med* 2017;**9**: 430−47.